Development 122, 3981-3990 (1996)
Printed in Great Britain © The Company of Biologists Limited 1996
DEV1128

valentino: a zebrafish gene required for normal hindbrain segmentation

Cecilia B. Moens[1,*], Yi-Lin Yan[1], Bruce Appel[1], Allan G. Force[1] and Charles B. Kimmel[2]

[1]Institute of Neuroscience and [2]Department of Biology, University of Oregon, Eugene, OR 97403-1254, USA

*Author for correspondence (e-mail: moens@uoneuro.uoregon.edu)

SUMMARY

Mutational analysis can serve both to identify new genes essential for patterning embryonic development and to determine their functions. Here we describe the identification and phenotypic characterization of alleles of *valentino*, which we recovered in a genetic screen that sought to identify mutations in the zebrafish that disrupt region-specific gene expression patterns in the embryonic brain. *valentino* is required for normal hindbrain segmentation and the hindbrain of *valentino* mutant embryos is shortened by the length of one rhombomere. We demonstrate that *valentino* is required cell-autonomously in the development of rhombomeres 5 and 6, and propose that *valentino* functions in the subdivision and expansion of a common precursor region in the presumptive hindbrain into the definitive rhombomeres 5 and 6. These results provide genetic evidence for a two-segment periodicity in the hindbrain and suggest that this periodicity arises sequentially, through the specification and later subdivision of a two-rhombomere unit, or 'protosegment'.

Key words: zebrafish, hindbrain, segmentation, *valentino*, rhombomere

INTRODUCTION

The subdivision of a continuous embryonic field into reiterated segments is a mechanism for the generation of regional diversity that is used across animal phyla. Such a process is evident in the vertebrate hindbrain, whose complex organization is based upon the transient appearance of seven or eight segments, or rhombomeres, during embryogenesis (Vaage, 1969). Rhombomeres serve to organize subsequent patterns of neuronal differentiation and neural crest migration in the hindbrain, and thus determine the architecture, innervation and function of the vertebrate head (reviewed in Guthrie, 1995). Neural crest cells leave the presumptive hindbrain at particular rhombomeric levels to contribute to the cranial ganglia and pharyngeal arches, and motor neurons differentiating in particular rhombomere pairs innervate the pharyngeal arches with a 2:1 correspondence (Lumsden and Keynes, 1989; Lumsden et al., 1991). Cell lineage analysis has shown that rhombomeres constitute developmental compartments, since cells generally fail to cross rhombomere boundaries once they are formed (Birgbauer and Fraser, 1994).

Although the genetic mechanisms that bring about segmentation in the *Drosophila* embryo are well understood (Nüsslein-Volhard and Wieschaus, 1980; reviewed in Akam, 1987), less is known about the genetic control of segmentation in the vertebrate hindbrain. A number of lines of evidence have suggested that rhombomeres have a two-segment periodicity, in which alternating odd and even identities are overlain by the expression of *Hox* genes, which specify regional identity in rhombomere pairs (Keynes and Krumlauf, 1994). Transplantation experiments in the chick have shown that cells in alternate rhombomeres are more similar to one another in adhesive properties than they are to cells in adjacent rhombomeres (Guthrie and Lumsden, 1991; Guthrie et al., 1993), and there are several genes that are expressed in alternate rhombomeres, at least one of which, *Krox-20*, is required for the development of rhombomeres 3 and 5 (Wilkinson et al., 1989a; Schneider-Manoury et al., 1993; Swiatek and Gridley, 1993).

We have undertaken a genetic screen in the zebrafish to identify genes involved in brain regionalization, particularly in hindbrain segmentation. Screening by RNA in situ hybridization for mutations that disrupt the normal regional patterns of gene expression in the brain, we have identified three alleles of *valentino (val)*, an essential gene required for segmentation in the posterior hindbrain. Our analysis of *valentino* mutant embryos and of genetic mosaics leads us to propose that *valentino* is required for the expansion and subdivision of a specified region of the presumptive hindbrain, which we term a 'protosegment', into the definitive rhombomeres 5 and 6. In the absence of *valentino* function, this protosegment persists but, lacking a terminal rhombomere identity, it fails to form boundaries with flanking rhombomeres. Our findings suggest that hindbrain segmentation occurs sequentially, through the initial specification of protosegments that correspond to the two-segment units later defined by *Hox* gene expression, and their subsequent subdivision and expansion into the definitive rhombomeres.

MATERIALS AND METHODS

RNA in situ hybridization screening of haploid embryos

We screened haploid embryos (Streisinger et al., 1981) produced by the F_1 progeny of male fish that had been mutagenized with either *N*-ethyl-*N*-nitrosourea (ENU; Solnica-Krezel et al., 1994) or γ-rays (C. Walker and C. Kimmel, unpublished data). At 22 hours postfertilization (h), 10 embryos from each clutch were dechorionated and fixed

in 4% paraformaldehyde (PFA) in phosphate-buffered saline (PBS). Since we were interested in identifying mutations that subtly altered the patterning of the central nervous system, we fixed embryos that appeared morphologically normal under the dissecting microscope. We screened simultaneously for mutations that disrupted the expression patterns of six genes: *krox20* (Oxtoby and Jowett., 1993), *eng3* (Ekker et al., 1992), *shh* (Krauss et al., 1993), *lim5* (Toyama et al., 1995), *myoD* (Weinberg et al., 1996), and *dlx-2* (Akimenko et al., 1994), after determining that the expression patterns of each of these genes was essentially normal in wild-type haploid embryos. RNA in situ hybridizations were performed essentially as described (Oxtoby and Jowett, 1993), using a 10×10 array of baskets constructed with Beem capsules (size 00; Ted Pella) and silk mesh to transfer embryos between washes. After colour development, embryos were washed in PBS containing 0.1% Tween-20 (PBT) and were scored in PBT under a dissecting microscope.

PCR typing of *val^{b361}* embryos

We identified PCR-based markers that are closely linked to *valentino* using methods described previously (Postlethwait et al., 1994; C. Moens and M. Giorgianni, unpublished results). The *snail2* gene (Thisse et al., 1995) maps to linkage group (LG) 23 (Gates and Postlethwait, personal communication) approximately 0.5 cM distal to *val^{b337}*. *snail2* is deleted in *val^{b361}* and thus could be used to distinguish *val^{b361}* embryos from their wild-type siblings. The primers used to amplify the *snail2* gene were: 5′-CACTCCGAGGTGAAGAAGTACC-3′ and 5′-GTGGAATCAAAACAGGCACC-3′, which amplified a 175 bp fragment. As a control, we used primers that amplify an unlinked (LG17) gene, *nk2.2*. Following RNA in situ hybridization, individual embryos were lysed in 50 μl Thermopol buffer (New England Biolabs) and were treated with 1 mg/ml Proteinase K for 3 hours at 55°C followed by incubation at 98°C for 10 minutes. 8 μl of the resulting lysate was used for a single PCR reaction.

Mosaic analysis

val^{b337}/val^{b337} embryos were produced by crossing *val^{b337}/val^{+}* fish together, yielding wild-type and mutant embryos in a 3:1 ratio. In one set of experiments (schematized in Fig. 4A), embryos from such a cross were labeled at the 1- to 2-cell stage with a mixture of lysinated tetramethyl rhodamine-dextran (LRD) and lysine-fixable biotinylated dextran (Molecular Probes), and wild-type embryos from a cross between homozygous wild-type fish were labeled with fluorescein-dextran. Using methods previously described (Ho and Kane, 1990), cells from both types of donor were transplanted into the same unlabeled wild-type host embryo at the shield stage (6 h; Kimmel et al., 1995). In some experiments cells were transplanted heterochronically, from dome-stage (4.3 h) donors into shield-stage hosts, with the same results. Cells were transplanted into the region of the host embryo that gives rise to the hindbrain (Woo and Fraser, 1995), and host embryos were left to develop until 18-24 h, at which time the distribution of labeled cells in the host hindbrain was determined. The genotype of donor embryos was determined by visual inspection of the hindbrain at 18 h. In a second set of experiments (schematized in Fig. 4K), cells from labeled wild-type donor embryos were transplanted into unlabeled host embryos from a *val^{b337}/val^{+}* intercross. Host embryos were left to develop until 18 h, at which time they were genotyped and the distribution of wild-type cells was determined. The distribution of labeled cells in live embryos was recorded using a Zeiss 310 confocal microscope and images were pseudocoloured using Voxelview 3-dimensional imaging software running on an Indigo 2XZ silicon graphics computer. For the repeated observation of mosaic embryos over time, transplanted cells were visualized using a low light-level silicon-intensified camera (Videoscope) and images were obtained using AxoVideo imaging software running on a Macintosh Quadra 950 computer.

Host embryos were fixed in 4% PFA between 20 and 28 h, and whole-mount RNA in situ hybridizations were performed as described above. In order to detect the donor-derived cells after RNA in situ hybridization, host embryos were re-fixed overnight, then processed for biotin detection using either avidin conjugated to horse-radish peroxidase (Fig. 4D-F; Vector Laboratories, Inc.) or avidin conjugated to Texas Red (Fig. 4L,M; Molecular Probes).

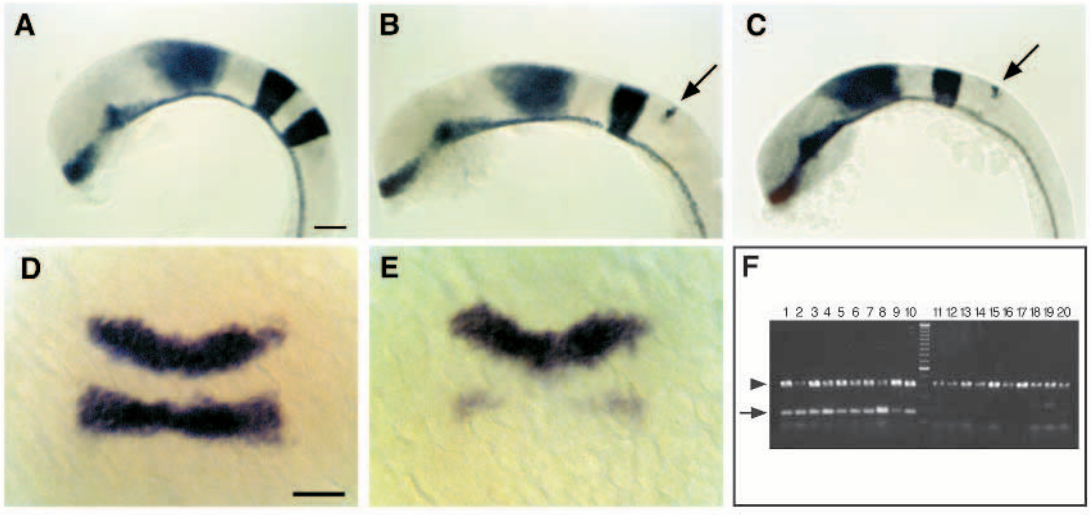

Fig. 1. *krox20* expression is disrupted in *val*$^{-}$ embryos early during hindbrain development. We screened 472 ENU-mutagenized and 741 γ-ray-mutagenized haploid genomes, and identified three alleles of *valentino*, one ENU-induced (*val^{b337}*) and two γ-ray-induced (*val^{b361}* and *val^{b475}*). (A-C) Whole-mount RNA in situ hybridizations in lateral view showing expression of three genes, *shh*, *en3* and *krox20*, in 18 h wild-type (A), *val^{b337}* (B) and *val^{b361}* (C) embryos. Anterior is to the left. In both alleles of *valentino* shown here, the r5 stripe of *krox20* staining is reduced to a vestigial strip of expression in the dorsal hindbrain at the position of the r4-r5 boundary (arrow). (D,E) Dorsal views of whole-mount RNA in situs showing expression of *krox20* in wild-type (D) and *val^{b337}* (E) embryos at the 2- to 3-somite stage (10⅔- 11 h). Anterior is to the top. In *val*$^{-}$ embryos, *krox20* expression is already disrupted in the presumptive r5. (F) Following RNA in situ hybridization at the 2- to 3-somite stage, embryos from a cross between *val^{b361}/val^{+}* individuals were sorted based on *krox20* expression and then their genotype was determined by PCR using *snail2*, which is deleted in *val^{b361}* (see Materials and Methods). 10/10 individuals scored as wild-type were in fact wild type as determined by PCR (lanes 1-10) and 10/10 individuals scored as mutant were in fact mutant (lanes 11-20). Arrow: *snail-2;* arrowhead: *nk2.2*, an unlinked gene that is amplified from both wild-type and mutant DNA. Scale bars, 50 μm.

Retrograde labeling of reticulospinal neurons

5-day larvae were anesthetized and mounted in a drop of 1% agar made in Ringer's solution. The tail was cut off at the level of the anus using spring scissors (Fine Science Tools) that had been dipped in a 5% solution of LRD. Retrograde fills from this level of the spinal cord are expected to result in labelling of the contralaterally projecting MiD2c and MiD3c cells but not of the ipsilaterally projecting MiD2i or MiD3i cells (Metcalfe et al., 1986). Larvae were removed from the agar and left to recover for 1 hour in Ringer's solution before being fixed overnight in 4% PFA. After fixation, the hindbrain was carefully removed, cleared stepwise in glycerol:PBS (50%, 70%, 90%), and mounted between 24×60 mm coverslips separated by the thickness of a single 22×22 mm coverslip. Images were obtained using a Zeiss 310 confocal microscope and were pseudocoloured using Voxelview 3-dimensional imaging software.

Antibody staining

16 μm cryostat sections were stained with the zn-5 antibody (Trevarrow et al., 1990) using the indirect peroxidase anti-peroxidase method (Hanneman et al., 1988).

RESULTS

Identification of *valentino*

We performed an RNA in situ hybridization screen of haploid zebrafish embryos to identify mutations that disrupt the region-specific expression patterns of several marker genes in the developing brain. Using this approach, we identified three independent mutations in which the rhombomere 5 (r5)-specific band of expression of *krox20*, a gene that is normally expressed in r3 and r5 (Oxtoby and Jowett, 1993), was reduced to a narrow strip of cells dorsal in the neural tube at the normal position of the r4-5 boundary (Fig. 1). Complementation tests and mapping showed that these mutations affect the same gene, which we named *valentino (val)*. The val^{b337} allele was identified among the haploid progeny of F_1 females from *N*-ethyl-*N*-nitrosourea (ENU)-mutagenized fish, and the val^{b361} and val^{b475} alleles were identified among the haploid progeny of F_1 females from γ-ray mutagenized fish. Both of the γ-ray-induced mutations are deletions and at least one of them, val^{b475}, constitutes a *valentino* deficiency since it deletes genetic markers on either side of *valentino* (C. Moens and M. Giorgianni, unpublished results).

All three *val* alleles are inherited in a Mendelian fashion as recessive lethal traits. Embryos homozygous for the ENU-induced allele die between 6 and 9 days after fertilization (d), by which time they are edemic and have failed to form a swim bladder. While the initial hindbrain defect caused by the γ-ray-induced mutations is identical to that caused by the ENU-induced mutation (see below), embryos homozygous for the γ-ray-induced mutations die by 3 d. Since the phenotype of *trans*-heterozygous embryos (val^{b361}/val^{b337} and val^{b475}/val^{b337}) is identical to that of embryos homozygous for the ENU-induced allele, we infer that the ENU-induced allele is a null allele of *valentino*, and that the earlier lethality caused by the γ-ray-induced mutations is due to the deletion of other essential genes (see Materials and Methods). Except where specifically noted, the analysis presented below is of the ENU-induced allele.

All three *val* alleles were identified due to the disruption of the r5-specific band of *krox20* expression described above. The r5-specific band of expression of *rtk1* (Xu et al., 1994) is similarly affected in val^{-} embryos (data not shown); however, the r1- and r3-specific bands of *rtk1*, the r3-specific band of *krox20*, as well as other markers of more anterior regions of the brain, are unaffected in val^{-} embryos (Fig. 1 and data not shown).

valentino is required early in the segmentation of the presumptive hindbrain, since the earliest known marker of segmentation, *krox20*, is already disrupted in val^{-} embryos at the early somite stages. As early as *krox20* expression is fully established in the presumptive r5, shortly after the end of gastrulation, it is reduced in 1/4 of the embryos produced in a cross between heterozygotes (Fig. 1). To determine whether the embryos showing reduced *krox20* expression in r5 at this stage were indeed val^{-}, embryos produced by crossing individuals heterozygous for the γ-ray-induced val^{b361} allele were sorted based on their *krox20* expression pattern at the 2- to 3-somite stage ($10\frac{2}{3}$-11 h), and then were genotyped by PCR using the linked marker *snail2*, which is deleted in this deficiency (M. Gates and J. Postlethwait, personal communication; C. Moens and M. Giorgianni, unpublished results). We found that, at this stage, val^{-} embryos could be reliably distinguished from their wild-type siblings based on *krox20* expression (Fig. 1F).

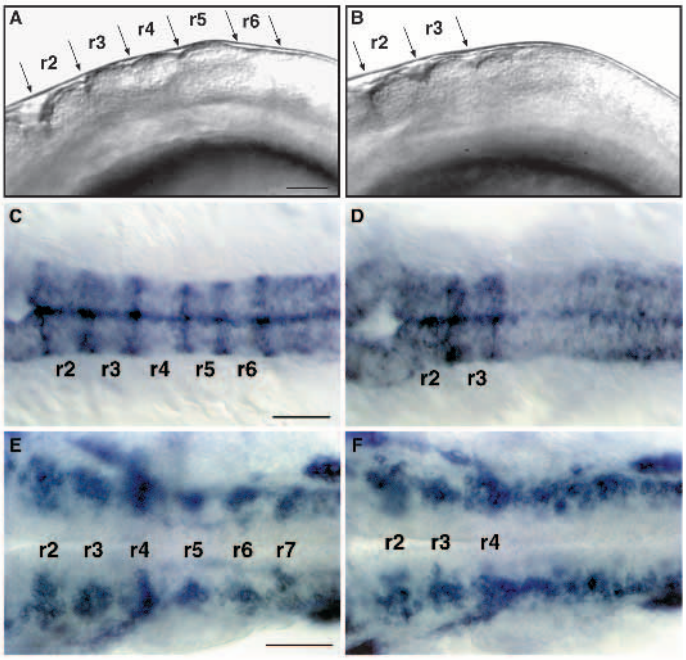

Fig. 2. val^{-} embryos lack segment boundaries and segmental patterns of neuronal differentiation posterior to rhombomere 4. (A,B) Lateral view of live 18 h wild-type (A) and val^{-} (B) embryos. Anterior is to the left. In val^{-} embryos, there are no visible rhombomere boundaries posterior to the r3-r4 boundary. (C,D) Dorsal views of RNA in situ hybridizations of wild-type (C) and val^{-} (D) embryos at 18 h showing expression of *mariposa* in the rhombomere boundaries. No expression is observed posterior to the r3-r4 boundary in val^{-} embryos. (E,F) Dorsal views of RNA in situ hybridizations of wild-type (E) and val^{-} (F) embryos at 24 h showing expression of *gap43* in clusters of early differentiating neurons laterally in each rhombomere. In val^{-} embryos, this segmental pattern of *gap43* staining is lost posterior to r4. This disrupted pattern of neuronal differentiation is also observed in val^{-} embryos stained with the HNK-1 antibody (data not shown; Metcalfe et al., 1990; Trevarrow et al., 1990). Scale bars, 50 μm.

Earlier than this, *val*⁻ embryos are more difficult to distinguish from wild types because the initiation of r5-specific *krox20* expression in two lateral domains (Oxtoby and Jowett, 1993) occurs to some extent in *val*⁻ embryos.

Hindbrain segmentation is disrupted in *valentino* mutants

Although *valentino* was originally identified by RNA in situ hybridization, live mutant embryos have a transiently visible phenotype during the period when rhombomeres are visible. In wild-type embryos at the 18-somite stage (18 h), r2 through r6 are visible as a series of prominent swellings, with the otic vesicle lying lateral to r5. In *val*⁻ embryos, the otic vesicle is reduced in size and no rhombomere boundaries are visible posterior to the r3/r4 boundary, giving the posterior half of the hindbrain a smooth appearance (Fig. 2A,B). The expression of *mariposa*, which is normally observed in rhombomere boundaries (Y. Yan and J. Postlethwait, unpublished results), is altered in *val*⁻ embryos in a manner that is consistent with this loss of visible rhombomere boundaries. *mariposa* expression is normally observed in six stripes in the hindbrain at 18 h. In *val*⁻ embryos, the three most posterior *mariposa* stripes, corresponding to the r4/5, r5/6 and r6/7 boundaries, are absent (Fig. 2C,D).

The segmental pattern of neuronal differentiation normally observed during hindbrain development (Trevarrow et al., 1990) is also disrupted in *val*⁻ embryos. Zebrafish *gap43* is expressed in a segmental pattern in the hindbrain at 24 h, in clusters of differentiating neurons that lie laterally in each rhombomere, as well as in the ganglia of the anterior and posterior lateral lines and trigeminal nerve (Fig. 2E; Reinhard et al., 1994). While clusters of differentiating neurons are visible in r2, r3 and r4 of *val*⁻ embryos, *gap43*-expressing cells posterior to r4 have lost their segmental organization (Fig. 2F). The disruption of segment boundaries and segmental patterns of neuronal differentiation posterior to r4 in *val*⁻ embryos suggests that *valentino* affects not only r5 but also more posterior regions of the hindbrain.

The hindbrain is reduced by the length of one rhombomere in *valentino* mutants

We used region-specific RNA probes to further investigate the *valentino* mutant phenotype. In wild-type embryos, the *headache (hdc)* gene is expressed in the spinal cord with a anterior boundary of expression at the r6/7 boundary (A. Force, C. Dunn and J. Postlethwait, unpublished results), and the *g13.1* gene is expressed in r4 and anterior to the r2-3 boundary (Fig. 3A; B. Appel and J. Eisen, unpublished results). Double RNA in situ hybridizations using these probes show that the hindbrain is reduced by the length of approximately one rhombomere in *val*⁻ embryos. In mutant embryos, the anterior boundary of *hdc* expression is shifted towards the *g13.1* domain of expression in r4, leaving a region of one rhombomere's length rather than two between r4 and r7. We term this single rhombomere-length unit 'rX' (Fig. 3B), and argue below that it corresponds to the domain that is normally subdivided and expanded into r5 and r6 in wild-type embryos. The expression boundaries of *hdc* and *g13.1*, which are normally quite sharp, are diffuse where they border rX in *val*⁻ embryos. This is consistent with the absence of rhombomere boundaries in this region of the hindbrain in *val*⁻ embryos. We note that localized cell death does not account for the observed reduction in hindbrain length in *val*⁻ embryos, since we observe no difference between wild-type and *val*⁻ embryos that were treated for the detection of programmed cell death at the 18-somite stage (data not shown; Gavrieli et al., 1992).

We examined the *valentino* mutant phenotype at the single cell level by determining the positions of identifiable neurons and neuronal cell types within the mutant hindbrain. The reticulospinal neurons are a series of individually identifiable neurons whose cell bodies form a ladder-like array corresponding to the positions of the rhombomeres and which can be visualized by the retrograde transport of lysinated rhodamine dextran from a spinal cord lesion (Kimmel et al., 1982; Metcalfe et al., 1986; Hanneman et al., 1988; see Materials and Methods). A subset of these (the 'primary' reticulospinal neurons) undergo their final division before the end of gastrulation (Mendelson, 1986) and transplantation experiments have revealed that they are committed to their particular segmental identities well before rhombomeres are visible (C. Moens, unpublished results). The most easily identifiable of the primary reticulospinal neurons are the large Mauthner neurons, which differentiate bilaterally in r4. Other identifiable primary reticulospinal neurons differentiate in characteristic positions in r3 (the RoM3 cells), r5 (the MiD2 cells), r6 (the MiD3 cells) and r7 (the CaD cell; Fig. 3C,D). The MiD2cm cell is characterized by its medial position, its rounded shape and its long, unbranched lateral dendrite (Fig. 3E). In contrast, the MiD3cm cell is characterized by its more lateral position, its fusiform shape and its shorter, branched lateral dendrite (Fig. 3F).

While the presence and position of these neurons are more variable in *val*⁻ than in wild-type embryos, we identified certain characteristic abnormalities (Fig. 3C-G; Table 1). The distance from the Mauthner (r4) cell to the CaD (r7) cell, which is characterized by its dorsal and medial position, its rounded shape and the extensive arborization of its ventral dendrite (not shown), is reduced on average to about 2/3 that observed in wild-type siblings, again demonstrating that the posterior hindbrain is reduced by one rhombomere in *val*⁻ embryos. Surprisingly, in light of the reduction of r5-specific gene expression, in most *val*⁻ embryos both the MiD2cm and MiD3cm cells are present and lie in the correct order. These

Table 1

	Wild-type		*val*⁻	
	Avg. dist. ± SD (μm)	n*	Avg. dist. ± SD (μm)	n
RoM3-Mth	32±3.1	15	33±5.3	26
Mth-MiD2	26±2.7	16	27±6.1	23
Mth-MiD3	62±3.9	15	38±11.8	22
Mth-CaD	90±5.1	14	58±10.0	27

*Refers to the number of unilateral measurements. Thus for one individual, n=2.

The presence or absence of each class of reticulospinal neuron was determined in 45 mutant and 17 wild-type individuals. In 3/45 mutant embryos examined, we observed a unilaterally duplicated Mauthner neuron caudal to the normal Mauthner neuron. Such an event is observed in less than 0.5% of wild-type embryos (Kimmel et al., 1978). In 11/45 mutant embryos examined, we observed a unilateral loss of MiD2 neurons (0/17 wild-type), and in 15/45 mutant embryos examined, we observed a unilateral loss of MiD3 neurons (0/17 wild-type).

cells lie close together in the shortened interval between the CaD cell and the Mauthner cell (Fig. 3D,G). This interval corresponds to rX in Fig. 3B.

The zn-5 antibody recognizes two clusters of efferent neurons that lie ventrally and medially in r5 and r6. Based on their position and axon projections, these neurons have been proposed to be the motor nuclei of the sixth (abducens) cranial nerve (Trevarrow et al., 1990). While these nuclei are easily identifiable in sagittal sections of zn-5-stained wild-type embryos at 3 days of development, they are rare or entirely absent in *val*$^{-}$ embryos, as are their characteristic anterior-projecting axons (Fig. 3H,I). The putative abducens motor nuclei differentiate relatively late during hindbrain development, since they first stain with zn-5 24 hours later than do the earlier differentiating hindbrain commissural neurons (Trevarrow et al., 1990). Thus, although the primary reticulospinal neurons characteristic of r5 and r6 are usually present in *val*$^{-}$ embryos, at least one later-differentiating cell type characteristic of r5 and r6 is absent.

Mosaic analysis shows that *valentino* is required for cells to contribute to r5 and r6

To determine which cells autonomously require *valentino* function during hindbrain development, we transplanted cells from labeled *val*$^{-}$ embryos into unlabeled wild-type hosts at the early gastrula stage (Fig. 4A; see Materials and Methods). As an internal control, we also transplanted cells from a wild-type donor labeled with a different fluorophor into the same wild-type host embryo. Both types of labeled cells were put into the region of the host gastrula that is fated to give rise to the hindbrain (Woo and Fraser, 1995), so that we could assess the distribution of mutant cells in the pharyngula-stage hindbrain (24 h). Wild-type cells contribute to the entire brain and spinal cord of wild-type hosts, where they form bilateral groups of cells that extend from the ventricular to the pial surface (Fig. 4B). In contrast, we observed that *val*$^{-}$ cells transplanted into the same wild-type host were specifically excluded from a sharply defined region in the hindbrain (Fig. 4C).

By identifying rhombomere boundaries in the mosaic embryos by RNA in situ hybridization using *krox20* or *mariposa* and detecting the donor-derived cells immunohistochemically, we determined that the region from which *val*$^{-}$ cells are excluded in mosaic embryos corresponds precisely to r5 and r6 (Fig. 4D-F). Thus *valentino* is required cell-autonomously for cells to contribute to either r5 or r6, suggesting that in the mutant itself there is no region with true r5 or r6 identity. We often observed mutant cells lying unilaterally or bilaterally at the r5-r6 boundary in wild-type host embryos (Fig. 4C,E,F).

In order to understand how *val*$^{-}$ cells come to be excluded from r5 and r6 of a wild-type host, we followed their behaviour over time following transplantation. As early as the 7-somite stage (12.5 h), *val*$^{-}$ cells were observed to disperse from the presumptive r5 and r6, contributing instead to the flanking rhombomeres (Fig. 4G). Mutant cells retracted first toward the lateral surface of the neural keel, and then gradually parted, leaving behind any cells that lay at the presumptive r5-6 boundary (Fig. 4H-J). Transplanted *val*$^{-}$ cells in the presumptive r5 and r6 failed to complete a characteristic division across the midline that normally occurs at cell cycle 16 and generates bilateral pairs of sister cells (Kimmel et al., 1994), but neither did they undergo cell death, which is visible in mosaic embryos by the appearance of brightly labelled flecks of debris. Thus *val*$^{-}$ cells appear to respond to the newly specified r5 and r6 environments in a wild-type host by selective dispersal rather than by selective cell death.

In the converse transplant experiment (schematized in Fig. 4K), wild-type cells contribute normally to the brain and spinal cord of *val*$^{-}$ host embryos except when they lie in rX (Fig. 4L). Wild-type cells lying in rX do not extend from the pial surface to the ventricular surface of the hindbrain, and fail to divide across the midline, instead forming unilateral clumps of rounded cells that appear to segregate away from the host cells. This characteristic behaviour suggests that wild-type cells lying in rX have a distinct identity from the surrounding mutant cells. Often clusters of wild-type cells come to lie at either end of rX, where rX borders r4 and r7. In these cases, clusters of wild-type cells lying ventral to the vestigial strip of *krox20* expression that marks the anterior end of rX express *krox20*, while the surrounding mutant cells do not (Fig. 4M). Thus, in a mutant host embryo, wild-type cells respond to signals that specify r5 identity by autonomously expressing r5-specific markers.

DISCUSSION

We devised an RNA in situ hybridization screen in the zebrafish to identify mutations that disrupt the normal segmental patterns of marker gene expression in the embryonic brain. Three alleles of *valentino* were identified in this screen by their lack of all but a narrow dorsal strip of *krox20* expression in r5. Mutations in *valentino* disrupt *krox20* expression from the earliest time that it is established in r5 and result in the absence of visible rhombomere boundaries and boundary-specific gene expression posterior to the r3-4 boundary. The normal segmental pattern of neuronal differentiation observed in the zebrafish hindbrain is also disrupted posterior to r4 in *val*$^{-}$ embryos, consistent with experiments in the chick that showed that, in the absence of rhombomere boundaries, cell mixing occurred between adjacent rhombomeres (Guthrie et al., 1993). In as much as it disrupts the process of segmentation itself, *valentino* is one of the relatively small number of genes, including *krox20*, *Hoxa-1* and *kreisler*, that have been shown to be required for hindbrain segmentation in the mouse (Schneider-Maunoury et al., 1993; Swiatek and Gridley, 1993; reviewed in Wright, 1993; also see below). Based on our analysis of marker gene expression, of the positions of identified neurons and of genetic mosaics, we propose that *valentino* is required cell-autonomously in a process whereby a distinct region of the presumptive hindbrain that we call a 'protosegment' corresponding to a two-rhombomere unit is subdivided and expanded into the definitive rhombomeres 5 and 6 (Fig. 5).

'rX': a distinct region in the *val*$^{-}$ hindbrain that fails to be subdivided and expanded into r5 and r6

The domains of marker gene expression and the positions of the primary reticulospinal neurons indicate that the distance between r4 and r7 is reduced from two rhombomere lengths to one in *val*$^{-}$ embryos (summarized in Fig. 5). 'rX' is the region that remains between, and fails to form boundaries with, r4 and

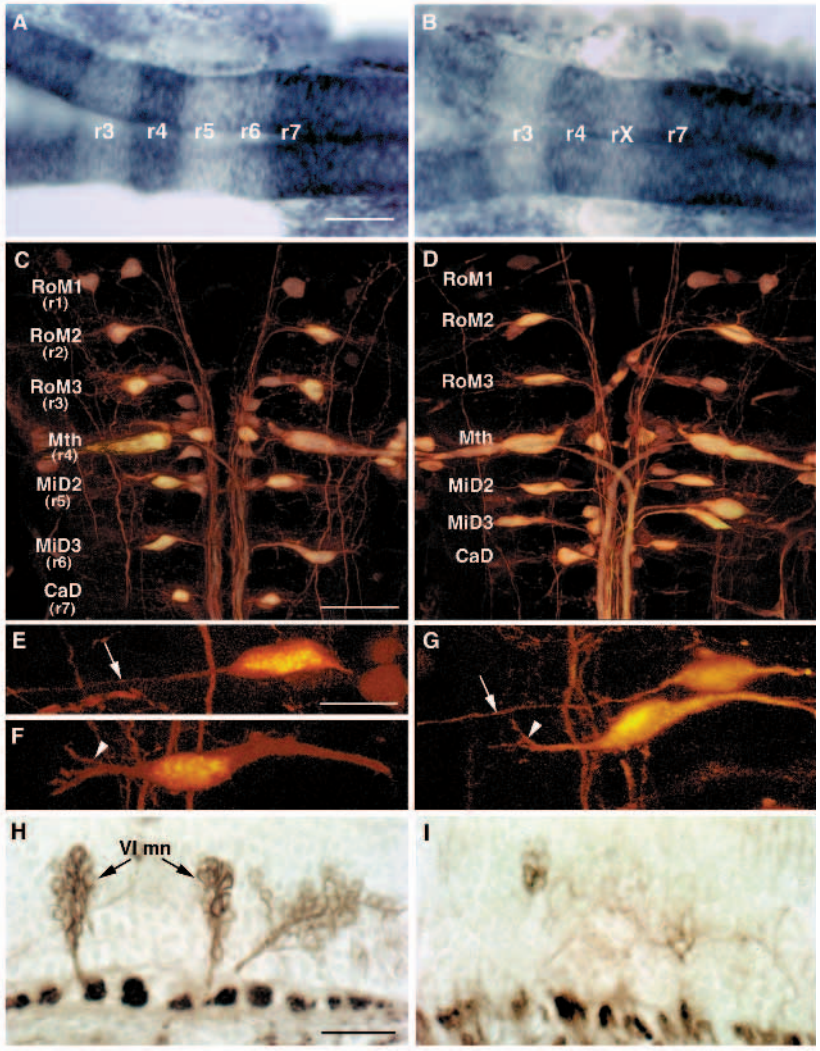

Fig. 3. The hindbrain of *val*⁻ embryos is reduced by the length of one rhombomere. (A,B) Dorsal view of 22 h wild-type (A) and *val*⁻ (B) embryos showing expression of two genes: *g13.1* in r4 and anterior to the r2-r3 boundary and *hdc* posterior to the r6-r7 boundary. Anterior is to the left. The distance between the posterior boundary of *g13.1* expression in r4 and the anterior boundary of *hdc* expression is reduced by the length of approximately one rhombomere in the *val*⁻ compared to the wild-type embryo. 'rX' refers to the region of that remains between r4 and r7. (C-G) Confocal images of 5-day old wild-type (C,E,F) and *val*⁻ (D,G) embryos in which the hindbrain reticulospinal neurons are visualized by retrograde filling with lysinated rhodamine-dextran. Anterior is to the top. The names of individually identifiable neurons are indicated. In wild-type embryos, the RoM3 neurons lie in r3, Mauthner (Mth) in r4, MiD2 in r5, MiD3 in r6 and CaD in r7. In *val*⁻ embryos, the average distance from Mth to CaD is reduced by the length of approximately one rhombomere, and the MiD2 and MiD3 neurons lie close together in the region of one rhombomere's length between r4 and r7. (E-G) Higher power confocal images of MiD2 and MiD3 cells in wild-type (E,F) and mutant (G) embryos. Arrows indicate the long, unbranched lateral dendrite characteristic of the MiD2cm cell, while arrowheads indicate the shorter, branched lateral dendrite characteristic of the MiD3cm cell. Note that, although the MiD2cm and MiD3cm cells are immediately adjacent to one another in the mutant embryo shown in G, the MiD2cm cell is still anterior to the MiD3cm cell. (H,I) Sagittal sections of 56 h wild-type (H) and *val*⁻ (I) embryos stained with the zn-5 antibody, which labels the putative motor nuclei of the abducens nerve (VI) in rhombomeres 5 and 6. Anterior is to the left. These motor nuclei are largely absent in the *val*⁻ embryo. The putative abducens motor nuclei differentiate relatively late during hindbrain development, since they first stain with zn-5 24 hours later than do the earlier differentiating hindbrain commissural neurons (Trevarrow et al., 1990). Scale bars, (A,B) 50 μm; (C,D) 50 μm; (E-G) 20 μm; (H,I) 20 μm.

r7. That this region is neither r5 *nor* r6, but has a distinct identity is suggested by a number of lines of evidence. rX does not express r5-specific markers except in a narrow strip of dorsal cells at the position where the r4-5 boundary would normally form. Thus rX is not r5. However, the MiD2 reticulospinal neuron, characteristic of r5, is generally found in rX of *val*⁻ embryos. As in the wild type, it lies anterior to the MiD3 reticulospinal neuron, which is characteristic of r6. We observe that later-differentiating r5- and r6-specific cell types are absent in *val*⁻ embryos, as indicated by the absence of the clusters of zn-5-positive cells which are the putative motor nuclei of the sixth (abducens) cranial nerve. Thus rX has some but not all of the characteristics of both r5 and r6. That the MiD2 and MiD3 neurons are generally present and lie in the correct order along the anterior-posterior axis of *val*⁻ embryos, if not in their correct positions, indicates that their specification is *valentino*-independent. It is even possible that they are specified before *valentino* functions: primary reticulospinal neurons are generated very early, before the end of gastrulation (Mendelson, 1986), and transplant experiments have shown that they are committed to their segment-specific identities before rhombomeres are visible (C. Moens, unpublished results).

The idea that rX of *val*⁻ embryos is distinct from either r5 or r6 is strongly supported by our analysis of genetic mosaics (Fig. 4). When cells from a *val*⁻ embryo at the early gastrula stage are transplanted into a wild-type embryo at the same stage and the mosaic embryo is allowed to develop, mutant cells are specifically excluded from r5 and r6. Meanwhile, wild-type cells transplanted into the same wild-type host contribute to the entire brain and spinal cord. Thus *valentino* is required cell-autonomously for cells to contribute to r5 and r6, suggesting that in the mutant embryo itself, there is no region with either r5 or r6 identity. Autonomy suggests that, in the mutant embryo, cells fail to respond normally to regional differences that are necessary for the specification of r5 and r6. That such regional differences do exist in *val*⁻ embryos is supported by our analysis of genetic mosaics in which wild-type cells are transplanted into a *val*⁻ host. We observe that clusters of wild-type cells lying at the anterior end of rX in *val*⁻ embryos express the r5-specific marker *krox20*, but clusters lying at the posterior end of rX do not. We predict that these

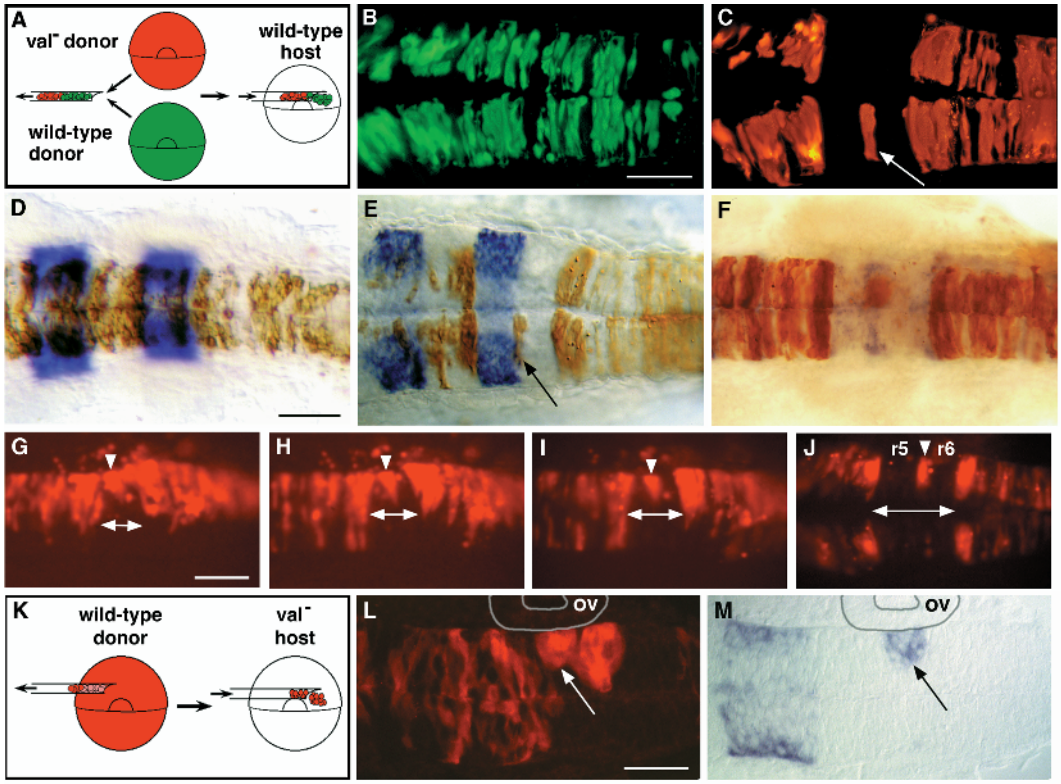

Fig. 4. Mosaic analysis demonstrates that *valentino* is required for cells to contribute to either r5 or r6. (A) Schematic diagram of the experimental approach used for B-J. Rhodamine-labeled cells from a *val*$^{-}$ donor and fluorescein-labeled cells from a wild-type donor were transplanted into the same unlabeled wild-type host at the early gastrula stage (see Materials and Methods). The distribution of labeled cells was then observed at 24 h of development. (B,C) Confocal images taken in dorsal view showing the distribution of wild-type (B) and *val*$^{-}$ cells (C) in the hindbrain region of the same wild-type host. *val*$^{-}$ cells are specifically excluded from a sharply defined region of the hindbrain, but are otherwise able to contribute to the entire brain and spinal cord. A single *val*$^{-}$ cell or small cluster of *val*$^{-}$ cells is frequently observed at the center of this region (arrow in C). (D-F) *krox20* staining (D,E) and *mariposa* staining (F) of transplant recipients. Brown cells are donor-derived (see Materials and Methods). (D) The distribution of wild-type cells in the hindbrain of a wild-type host. (E,F) The distribution of *val*$^{-}$ cells in a wild-type host, showing that mutant cells are specifically excluded from r5 and r6. The embryo shown in E is the same embryo as is shown in B and C, and the cell noted in C is observed to lie at the r5-6 boundary (arrow in E). In 31 out of 39 genetically mosaic embryos analyzed in which transplanted cells had contributed to the hindbrain, labelled *val*$^{-}$ cells were excluded from r5 and r6 although not necessarily from the boundary between them. In the remaining 8 mosaic embryos, *val*$^{-}$ cells were observed in r5 and/or r6, but these cells were located ventrally, either in or very near the floor plate (not shown). In contrast, 94 out of 100 control embryos into which labeled wild-type cells had been transplanted had labeled cells distributed throughout the hindbrain, including r5 and r6. The remaining 6 control embryos had relatively few transplanted cells and these tended to be localized to rhombomere boundaries. (G-J) A series of live images of rhodamine-labeled *val*$^{-}$ cells transplanted into a single wild-type host, shown in dorsal view. The time-points shown are 7 somites (12 h; G), 10 somites (14 h; H), 14 somites (16 h; I) and 24 h (J). As early as the 7-somite stage, *val*$^{-}$ cells begin to be excluded from the presumptive r5 and r6 of a wild-type host (indicated by a double arrow at the midline), with the exception of a few cells that ultimately lie at the r5-6 boundary (arrowheads). (K) Schematic diagram of the experimental approach used for L and M. Rhodamine-labeled cells from a wild-type donor were transplanted into a *val*$^{-}$ host embryo at the early gastrula stage. (L,M) Fluorescent and transmitted light images of the same horizontal section of a mutant host embryo. Anterior is to the left. Donor-derived cells in this experiment are fluorescently labelled. (L) Wild-type cells in a *val*$^{-}$ host form abnormal, unilateral clusters of rounded cells in rX, which is adjacent to the otic vesicle (ov), while they otherwise contribute normally to the brain and spinal cord. (M) The more anterior of these clusters, which lies at the r4-rX boundary, autonomously expresses *krox20* although the surrounding mutant cells have failed to acquire r5 identity (arrow in L and M). Scale bars: B,C, 100 μm; D-F, 50 μm; G-J, 100 μm; L,M, 50 μm.

posterior clusters instead express r6-specific markers. In these experiments, wild-type cells always segregate from the surrounding mutant cells in rX, indicating that their newly acquired r5 or r6 identity is incompatible with that of rX.

What, then, is the identity of rX? We propose that during normal development, a defined region or 'protosegment' in the presumptive hindbrain is subdivided and expanded into the definitive rhombomeres r5 and r6 (Fig. 5A). In the absence of *valentino*, this protosegment fails to be subdivided into r5 and r6, and fails to be expanded from one rhombomere's length to two, persisting instead as rX (Fig. 5B). We propose that rX identity, although distinct, is earlier in a hierarchy of regional identities than that of a definitive rhombomere. Thus rX is neither 'even' nor 'odd'. Consistent with experiments in the chick that showed that boundary formation between adjacent rhombomeres requires an even-odd distinction (Guthrie and Lumsden, 1991), rX fails to form boundaries, either morphologically visible or as detected by *mariposa* expression, with r4 and r7.

Further analysis of the *valentino* gene will reveal more precisely how it functions in the subdivision and expansion of r5 and r6 from their common precursor protosegment. Our results suggest that anterior-posterior differences exist within the protosegment independent of *valentino*, but that *valentino* is required within the protosegment for cells to respond to these differences by differentiating along r5- or r6-specific pathways. The *valentino* gene product could be required in the reception or transduction of signals that specify these differences, or

could act in concert with the products of genes that specify these differences, to drive r5- and r6-specific transcription. Alternatively, *valentino* could be required for cells in the protosegment to become competent to respond to these differences.

valentino mutant cells are excluded from wild-type r5 and r6 by selective dispersal, not selective cell death

The inability of *val*$^-$ cells to respond to regional differences that specify r5 and r6 results in their exclusion from r5 and r6 in genetic mosaics. Beginning at approximately the 7-somite stage (12.5 h), *val*$^-$ cells begin to be excluded from the presumptive r5 and r6, migrating instead into the flanking rhombomeres. Once there, they intercalate normally with the wild-type host cells, suggesting that *valentino* is not required for cells to take on r4 or r7 identity, and that *val*$^-$ cells remain uncommitted with respect to rhombomere identity until they encounter signals to which they can respond. Thus the exclusion of *val*$^-$ cells from r5 and r6 involves selective cell dispersal. These types of differential cell movements are reminiscent of those observed when cells were transplanted between odd- and even-numbered rhombomeres in the chick (Guthrie et al., 1993). These experiments suggested that differential adhesiveness between cells from adjacent rhombomeres could provide a mechanism for the maintenance of rhombomere boundaries (Guthrie and Lumsden, 1991; Guthrie et al., 1993). However, we observe this selective dispersal of cells with different regional identities in our genetic mosaics well before the appearance of visible rhombomere boundaries, which occurs at about the 14-somite stage (16 h). Thus differential adhesiveness between cells with different regional identities may exist earlier than this mechanism has been proposed to account for the restriction of cell movement between rhombomeres in the chick (Guthrie and Lumsden, 1991; Guthrie et al., 1993).

Timing of *valentino* function

Mutant cells appear to move out of the presumptive r5 and r6 of a wild-type host beginning at about the 7-somite stage, but *valentino* function is already required 1.5 hours earlier, when a disruption of the r5-specific expression of *krox20* is first detected in *val*$^-$ embryos. This difference may be artifactual since earlier movement by some of the many *val*$^-$ cells initially present in the presumptive r5 and r6 may not have been detected at our level of resolution. The difference may also reflect a delay between the specification of rhombomere identity and the acquisition of cell surface properties that prevent cells with different regional identities from mixing. It is also possible, however, that *val*$^-$ cells acquire r5 and r6 identity in a wild-type host but fail to maintain it, allowing them to contribute transiently to the presumptive r5 and r6. Indeed, *valentino* is not required for the initiation of r5-specific *krox20* expression, which occurs shortly before the 1-somite stage, since wild-type and *val*$^-$ embryos cannot be distinguished based on *krox20* expression until the 2- to 3-somite stage. This brief wave of *valentino*-independent r5 and r6 identity in *val*$^-$ embryos may be sufficient to specify the MiD2 and MiD3 primary reticulospinal neurons, which have undergone their final division by this time (Mendelson, 1986).

Similarities between *valentino* and *kreisler* mutants

The *val*$^-$ phenotype is reminiscent of that of the mouse mutant, *kreisler*, first described by Hertwig (1944). Like *valentino*, *kreisler* mutant embryos lack morphological segmentation in the hindbrain posterior to the r3-4 boundary (Deol, 1964). The mouse *kreisler* gene has been cloned (Cordes and Barsh, 1994), and we have evidence that *valentino* is its zebrafish homolog (C. Moens and S. Cordes, unpublished results). In spite of striking similarities between the *kreisler* and *valentino* mutant phenotypes, our interpretation of the *valentino* phenotype differs from either of the current interpretations of the *kreisler* phenotype (Cordes and Barsh, 1994; McKay et al., 1994). Both of these studies propose that the *kreisler* hindbrain consists of some combination of definitive rhombomeres. In contrast, our results suggest that in the *valentino* hindbrain r5 and r6 are

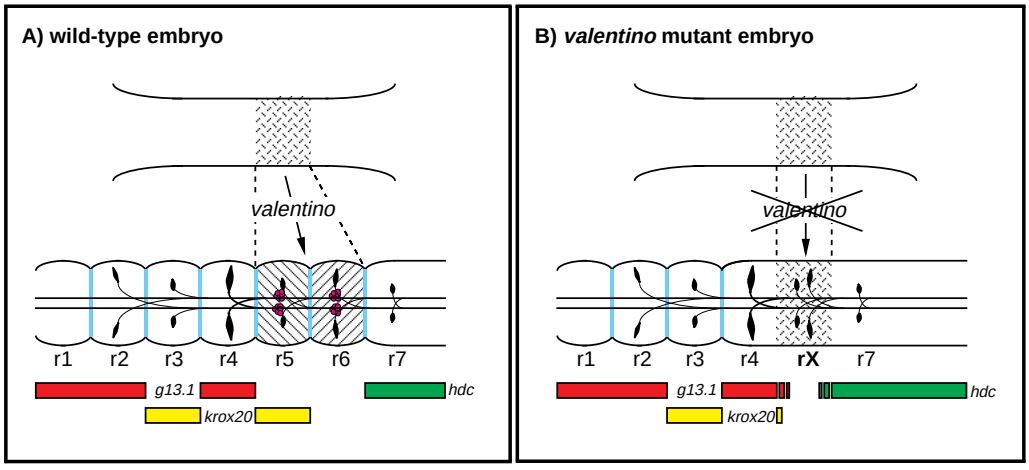

Fig. 5. Model for the function of *valentino* in hindbrain segmentation. In the wild-type embryo (A), *valentino* is required for the subdivision and expansion of a defined region (or protosegment) in the presumptive hindbrain (stippled area), into rhombomeres 5 and 6, whose identities are distinct from that of the protosegment (hatched rather than stippled) and from each other (left hatches versus right hatches). In the mutant embryo (B), this subdivision fails to happen and, as a result, the protosegment persists as rX. In the genetic mosaics, mutant cells are excluded from both r5 and r6 of a wild-type host because they are unable to make the transition from protosegment identity to r5 or r6 identity, and, conversely, wild-type cells behave abnormally in rX of a mutant host because they have acquired an identity (r5 or r6) which the surrounding mutant cells have failed to acquire. Coloured bars indicate the domains of expression of *krox20* (yellow), *hdc* (green) and *g13.1* (red), and the blue vertical lines at the rhombomere boundaries indicate *mariposa* expression. The average positions of the primary reticulospinal neurons are shown (black cells), as are the positions of the putative abducens motor nuclei (pink).

replaced by a region of one rhombomere's length that has a distinct and developmentally earlier identity than any definitive rhombomere.

Two-segment repeats

The patterns of neuronal differentiation, pharyngeal arch innervation and neural crest migration observed in the chick suggested the existence of a two-segment periodicity in the hindbrain (Lumsden and Keynes, 1989; Lumsden et al., 1991). Transplantation experiments in the chick have supported this hypothesis by showing that cells from alternate rhombomeres are more similar to each other in adhesive properties than they are to cells from adjacent rhombomeres (Guthrie and Lumsden, 1991; Guthrie et al., 1993). A two-segment periodicity is also suggested by the observation that a number of genes, such as *krox20*, *rtk1* and others, are expressed in alternate rhombomeres (Wilkinson et al., 1989a; Xu et al., 1994). Indeed, *krox20* is required for the formation of two alternate rhombomeres, r3 and r5, in the mouse (Schneider-Maunoury et al., 1993; Swiatek and Gridley, 1993). Furthermore, the anterior boundaries of 3′-*Hox* gene expression largely conform to a two-segment periodicity (Wilkinson et al., 1989b; reviewed in Keynes and Krumlauf, 1994).

Kimmel et al. (1985) noted a 2:1 correspondence between the 'segments' defined by the positions of the cranial nerves and the segments defined by the reticulospinal neurons, and suggested that neuromeres may originally have been assembled by a process of serial duplication (see also Stern, 1990). Our interpretation of the *val*$^{-}$ phenotype and of the results of our mosaic analysis support a model whereby segmentation occurs hierarchically, with the hindbrain being divided into protosegments corresponding to two-rhombomere units which are then subdivided and expanded into the definitive rhombomeres. The evidence presented here demonstrates such a process at work in the generation of rhombomeres 5 and 6, and it is possible that other, as-yet unidentified, genes function in an analogous manner to *valentino* in other rhombomere pairs.

Vaage (1969) noted that hindbrain segmentation in the chick occurred progressively, by the subdivision of three morphologically visible 'prorhombomeres'. However the two-rhombomere unit in which *valentino* functions does not correspond either to Vaage's prorhombomere B, which is subdivided into r4 and r5, or prorhombomere C, which is subdivided into r6 and r7. It may be that the timing of visible segmentation does not necessarily correspond to the timing of rhombomere specification. Interestingly, the two-rhombomere unit within which *valentino* functions does correspond to the two-rhombomere units defined by *Hox* gene expression (Keynes and Krumlauf, 1994). Mutations in *valentino* disrupt expression of *krox20*, which is known in turn to regulate *Hox* gene expression (Sham et al., 1993; Nonchev et al., 1996). Taken together, these results suggest that *valentino* functions to regulate *Hox* gene expression in the presumptive r5 and r6.

We wish to thank Sharon Amacher for her help with the mosaic analysis, and Will Talbot, Jim Langeland, Sharon Amacher, Bill Jackman, Bill Trevarrow, John Postlethwait, Judith Eisen and Victoria Prince for their helpful comments on the manuscript. C. B. M. was supported by a Natural Sciences and Engineering Research Council of Canada Postdoctoral Fellowship and a Human Frontier Science Program Long Term Fellowship. This work was supported by NIH grants NS17963, NS23915, HD22486 and RR10715.

REFERENCES

Akam, M. (1987). The molecular basis for metameric pattern in the *Drosophila* embryo. *Development* **101**, 1-22.

Akimenko, M. A., Ekker, M., Wegner, J., Lin, W. and Westerfield, M. (1994). Combinatorial expression of three zebrafish genes related to *distal-less*: part of a homeobox gene code for the head. *J. Neurosci.* **14**, 3475-3486.

Birgbauer, E. and Fraser, S. E. (1994). Violation of cell lineage restriction compartments in the chick hindbrain. *Development* **120**, 1347-1356.

Cordes, S. P. and Barsh, G. S (1994). The mouse segmentation gene *kr* encodes a novel basic domain-leucine zipper transcription factor. *Cell* **79**, 1025-1034.

Deol, M. S. (1964). The abnormalities of the inner ear in *kreisler* mice. *J. Embryol. Exp. Morph.* **12**, 475-490.

Ekker, M., Wegner, J., Akimenko, M. A. and Westerfield, M. (1992). Coordinate embryonic expression of three zebrafish engrailed genes. *Development* **116**, 1001-1010.

Gavrieli, Y., Sherman, Y. and Ben-Sasson, S. A. (1992). Identification of programmed cell death in situ via specific labeling of nuclear DNA fragmentation. *J. Cell. Biol.* **119**: 493-501.

Guthrie, S. and Lumsden, A. (1991). Formation and regeneration of rhombomere boundaries in the developing chick hindbrain. *Development* **112**, 221-229.

Guthrie, S., Prince, V. and Lumsden, A. (1993). Selective dispersal of avian rhombomere cells in orthotopic and heterotopic grafts. *Development* **118**, 527-538.

Guthrie, S. (1995). The status of the neural segment. *Trends Neurosci.* **18**, 74-79.

Hanneman, E., Trevarrow, B., Metcalfe, W. K., Kimmel, C. B. and Westerfield, M. (1988). Segmental pattern of development of the hindbrain and spinal cord of the zebrafish embryo. *Development* **103**, 49-58.

Hertwig, P. (1944). Die Genese der Hirn-und Gehörorganmißbildungen bei rontgenmutierten Kreislermäusen. *Z. KonstLehnre* **28**, 327-354.

Ho., R. K. and Kane, D. A. (1990). Cell-autonomous action of zebrafish *spt-1* mutation in specific mesodermal precursors. *Nature* **348**, 728-730.

Keynes, R. and Krumlauf, R. (1994). *Hox* genes and the regionalization of the nervous system. *Annu. Rev. Neurosci.* **17**, 109-132.

Kimmel, C. B., Sessions, S. K. and Kimmel, R. J. (1978). Radiosensitivity and time of origin of Mauthner neuron in the zebrafish. *Dev. Biol.* **62**, 526-529.

Kimmel, C. B., Powell, S. L. and Metcalfe, W. K. (1982). Brain neurons which project to the spinal cord in young larvae of the zebrafish. *J. Comp. Neurol.* **205**, 112-127.

Kimmel, C. B., Metcalfe, W. K. and Schabtach, E. (1985). T reticular interneurons: a class of serially repeating cells in the zebrafish hindbrain. *J. Comp. Neurol.* **233**, 365-376.

Kimmel, C. B., Warga, R. M. and Kane, D. A. (1994). Cell cycles and clonal strings during formation of the zebrafish central nervous system. *Development* **120**, 265-276.

Kimmel, C. B., Ballard, W. W., Kimmel, S. R., Ullmann, B. and Schilling, T. F. (1995). Stages of embryonic development of the zebrafish. *Dev. Dyn.* **203**, 253-310.

Krauss, S., Concordet, J. P. and Ingham, P. W. (1993). A functionally conserved homolog of the Drosophila segment polarity gene *hh* is expressed in tissues with polarizing activity in zebrafish embryos. *Cell* **75**, 1431-1444.

Lumsden, A. and Keynes, R. (1989). Segmental patterns of neuronal development in the chick hindbrain. *Nature* **337**, 424-428.

Lumsden, A., Sprawson, N. and Graham, A. (1991). Segmental origin and migration of neural crest cells in the hindbrain region of the chick embryo. *Development* **113,** 1281-1291.

McKay, I. J., Muchamore, I., Krumlauf, R., Maden, M., Lumsden, A. and Lewis, J. (1994). The *kreisler* mouse: a hindbrain segmentation mutant that lacks two rhombomeres. *Development* **120**, 2199-2211.

Mendelson, B. (1986). Development of reticulospinal neurons of the zebrafish. I. Time of Origin. *J. Comp. Neurol.* **251**, 160-171.

Metcalfe, W. K., Mendelson, B. and Kimmel, C. B. (1986). Segmental homologies among reticulospinal neurons in the hindbrain of the zebrafish larva. *J. Comp. Neurol.* **251**, 147-159.

Metcalfe, W. K., Myers, P. Z., Trevarrow, B., Bass, M. B. and Kimmel, C.

B. (1990). Primary neurons that express the L2/HNK-1 carbohydrate during early development in the zebrafish. *Development* **110**, 491-504.

Nonchev, S., Vesque, C., Maconochie, M., Seitanidou, T., Ariza-McNaughton, L., Frain, M., Marshall, H., Sham, M. H., Krumlauf, R. and Charnay, P. (1996). Segmental expression of *Hoxa-2* in the hindbrain is directly regulated by *Krox-20*. *Development* **122**, 543-554.

Nüsslein-Volhard, C. and Wieschaus, E. (1980). Mutations affecting segment number and polarity in *Drosophila*. *Nature* **287**, 795-801.

Oxtoby, E. and Jowett, T. (1993). Cloning of the zebrafish *krox-20* gene *(krx-20)* and its expression during hindbrain development. *Nucleic Acids Res.* **21**, 1087-1095.

Postlethwait, J. H., Johnson, S. L., Midson, C. N., Talbot, W. S., Gates, M., Ballinger, E. W., Africa, D., Andrews, R., Carl, T., Eisen, J. S., *et al.* (1994). A genetic linkage map for the zebrafish. *Science* **264**, 699-703.

Reinhard, E. Nedivi, E., Wegner, J., Skene, J. H. P. and Westerfield, M. (1994). Neural selective activation and temporal regulation of a mammalian GAP-43 promoter in zebrafish. *Development* **120**, 1767-1775.

Schneider-Maunoury, S., Topilko, P., Seitandou, T., Levi, G., Cohen-Tannoudji, M., Pournin, S., Babinet, C. and Charnay, P. (1993). Disruption of *Krox-20* results in alteration of rhombomeres 3 and 5 in the developing hindbrain. *Cell* **75**, 1199-1214.

Sham, M. H., Vesque, C., Nonchev, S., Marshall, H., Frain, M., Gupta, R. D., Whiting, J., Wilkinson, D., Charnay, P. and Krumlauf, R. (1993). The zinc finger gene *Krox20* regulates *HoxB2 (Hox2.8)* during hindbrain segmentation. *Cell* **72**, 183-196.

Solnica-Krezel, L., Schier, A. F. and Driever, W. (1994). Efficient recovery of ENU-induced mutations from the zebrafish germline. *Genetics* **136**, 1401-1420.

Streisinger, G., Walker, C., Dower, N., Knauber, D. and Singer, F. (1981). Production of clones of homozygous diploid zebra fish *(Brachydanio rerio)*. *Nature* **291**, 293-296.

Stern, C. D. (1990). Two distinct mechanisms for segmentation? *Seminars in Devel. Biol.* **1**, 109-116.

Swiatek, P. J. and Gridley, T. (1993). Perinatal Lethality and defects in hindbrain development in mice homozygous for a targeted mutation of the zinc finger gene *Krox20. Genes Dev.* **7**, 2071-2084.

Thisse, C., Thisse, B. and Postlethwait, J. H. (1995). Expression of *snail2*, a second member of the zebrafish *snail* family, in cephalic mesendoderm and presumptive neural crest of wildtype and *spadetail* mutant embryos. *Dev. Biol.* **172**, 86-99.

Toyama, R., Curtiss, P. E., Otani, H., Kimura, M., Dawid, I. B. and Taira, M. (1995). The LIM class homeobox gene *lim5*: implied role in CNS patterning in Xenopus and zebrafish. *Dev. Biol.* **170**, 583-593.

Trevarrow, B., Marks, D. L. and Kimmel, C. B. (1990). Organization of hindbrain segments in the zebrafish embryo. *Neuron* 4, 669-679.

Vaage, S. (1969). The segmentation of the primitive neural tube in chick embryos *(Gallus domesticus)*. *Adv. Anat. Embryol. Cell Biol.* **41**, 1-88.

Weinberg, E. S., Allende, M. L., Kelly, C. S., Abdelhamid, A., Murakami, T., Andermann, P., Doerre, O. G., Grunwald, D. J. and Riggleman, B. (1996). Developmental regulation of zebrafish *MyoD* in wildtype, *no tail* and *spadetail* embryos. *Development* **122**, 271-280.

Wilkinson, D. G., Bhatt, S., Cook, M., Boncinelli, E. and Krumlauf, R. (1989a). Segmental expression of Hox-2 homoeobox-containing genes in the developing mouse hindbrain. *Nature* **341**, 405-409.

Wilkinson, D. G., Bhatt, S., Chavrier, P., Bravo, R. and Charnay, P. (1989b). Segment-specific expression of a zinc-finger gene in the developing nervous system of the mouse. *Nature* **337**, 461-464.

Woo, K. and Fraser, S. E. (1995). Order and coherence in the fate map of the zebrafish nervous system. *Development* **121**, 2595-2609.

Wright, C. V. E. (1993). *Hox* genes and the hindbrain. *Current Biology* **3**, 618-621.

Xu, Q., Holder, N., Patient, R. and Wilson, S. W. (1994). Spatially regulated expression of three receptor tyrosine kinase genes during gastrulation in the zebrafish. *Development* **120**, 287-299.

(Accepted 4 September 1996)